JOURNAL OF THE KOREAN ASTRONOMICAL SOCIETY
31: 141 ~ 160, 1998

SURFACE PHOTOMETRY OF THREE SPIRAL GALAXIES : ESO 598-G009, NGC 1515 AND NGC 7456

CHOI, YOUNG-JUN[1,*], PARK, BYEONG-GON[1,2], YOON, TAE SEOG[1] AND ANN, HONG BAE[3]
[1]Department of Astronomy and Atmospheric Sciences, Kyungpook National University, Taegu 702-701
[2]Bohyunsan Optical Astronomy Observatory, Korea Astronomy Observatory, Kyungpook 770-820
[3]Department of Earth Sciences, Pusan National University, Pusan 609-735
(Received Oct. 1, 1998; Accepted Oct. 17, 1998)

ABSTRACT

We have conducted *BVRI* CCD surface photometry of three spiral galaxies ESO 598-G009, NGC 1515 and NGC 7456. In order to understand the morphological properties and luminosity distribution characteristics for each galaxy, we derived isophotal map, position angle profile, ellipticity profile, luminosity profile, color profile and color contour map. ESO 598-G009, which has a bright bulge component and a ring, shows a trace of gravitational interaction. NGC 1515 is a spiral galaxy with a bar and dust lane. NGC 7456 shows typical characteristics of a late type spiral galaxy.

Key Words : galaxies, surface photometry, structure, profile decomposition

I. INTRODUCTION

Surface photometry is a very useful method for understanding the structure and physical properties of galaxies. From the surface photometry, it has been known that the luminosity profile of elliptical galaxies follows de Vaucouleurs' $r^{1/4}$ law and the disk of spiral galaxies obeys exponential luminosity profile whose central surface brightness has a nearly uniform value of 21.65 ± 0.30 mag arcsec^{-2}(Freeman 1970).

The quantitative morphology, based on the decomposition of luminosity into distinct components, is initiated by Kormendy (1977b) who decomposed the luminosity profile of red compact galaxies into disk and bulge components, which follows Freeman's exponential law and de Vaucouleurs' $r^{1/4}$ law, respectively. Since Kormendy's pioneering work on the profile decomposition, there have been many attempts to understand the structure of spiral galaxies via quantitative morphology (Burstein 1979; Boroson 1981; Kent 1985; Simien and de Vaucouleurs 1986; Ann and Lee 1987), which lead to the understanding that structure of galaxies along Hubble sequence can be described as a function of the bulge-to-disk ratios.

The purpose of the present paper is to analyze the structure of three, relatively poorly studied spiral galaxies, ESO 598-G009, NGC 1515, and NGC 7456, by deep *BVRI* CCD surface photometry. The basic parameters of the program galaxies are given in Table 1.

ESO 598-G009 is a Sb(pec) type galaxy and its total blue magnitude is 14.26 in the Third Reference Catalogue of Bright Galaxies (de Vaucouleurs et al. 1991, hereinafter RC3). Using statistical analysis, Soares et al. (1995) suggested that ESO 598-G009 is an isolated pair which is a binary system with no companion inside the 1 Mpc circle. Mathewson et al. (1992, 1996) gave an information on inclination and heliocentric systemic velocity.

NGC 1515 is a highly elongated intermediate barred spiral galaxy, classified as SAB(s)bc in RC3. It has a very bright nucleus and two main arms. Total magnitude in blue band is 11.95.

NGC 7456 is a late type spiral galaxy, classified as SA(s)cd in RC3. Sandage and Brucato (1979) commented for this galaxy that there are a few HII regions and candidates.

The luminosity profiles for these galaxies were presented by Mathewson et al. (1992). However detailed surface photometry has not yet been performed for any of these galaxies.

The observations and the procedure of data reduction are described in section II. The isophotal maps, luminosity profiles and color profiles and the results of the profile decomposition are given in section III. A brief summary of the present study follows in the last section.

II. OBSERVATION AND DATA REDUCTION

The CCD frames were taken with the f/8 1-m Cassegrain reflector at the Mount Stromlo and Siding Spring Observatory (MSSSO) of Australia during a run in September 1993. The detector used was the TK1024 chip manufactured by Tektronix, Inc., with a format of 1024 × 1024 pixels. The physical size of a pixel is 24 μm square which gives the scale of 0.618 arcsec/pixel at the telescope. The more information about MSSSO 1m CCD observation system can be found in Park (1993).

We corrected the images with the Image Reduction

* Current address : Korea Astronomy Observatory

Table 1. Parameters of galaxies

	ESO 598-G009	NGC 1515	NGC 7456
R.A.(2000)	$20^h\ 58^m\ 28^s$	$4^h\ 4^m\ 3^s$	$23^h\ 02^m\ 10^s$
Dec(2000)	-19° 58' 55"	-54° 06' 10"	-39° 34' 9"
l, b	27.32, -36.59	264.1, -45.85	357.19, -64.16
Morphological type			
in RC3	Sb(pec)	SAB(s)bc	SA(s)cd
in RSA[a]	-	Sc II	Sc II-III
in ESO[b]	Sb	Sc	Sc
Diameters in ESO	1.5' x 0.6'	6.3' x 1.5'	8.0' x 2.6'
Position angle in ESO	145	18	23
R_{25} in RC3	0.39	0.67	0.53
b/a in ESO	0.4	0.24	0.33
Total magnitude(B_T)			
in RC3	14.26	11.95	12.18
in MCG[c]	14	-	12.5
$(B-V)_T$ in RC3	-	0.85	0.52
Inclination(degree)	62	81	70
Total magnitude	12.31	9.73	10.97

a : The Revised Shapley-Ames Catalog of Bright Galaxies (Sandage & Tammann, 1981)

b : The ESO/Uppsala Survey of the ESO(B) Atlas (Lauberts, 1982)

c : Morphological Catalogue of Galaxies (Vorontsov-Vel'yaminov, 1977)

and Analysis Facilities (IRAF), using standard techniques of bias subtraction and division by the normalized sky flat field. The reduction procedures for the surface photometry of a galaxy, which consist of several steps such as background sky subtraction, smoothing, cleaning, and absolute calibration, were performed by Surface Photometry Interactive Reduction and Analysis Library (SPIRAL) package along with IRAF, which was developed at Kiso observatory and implemented by Masaru Hamabe in Japan (Ichikawa *et al.*1987). The images of ESO 598-G009, NGC 1515 and NGC 7456 in B-band are shown in Figure 1.

We examine the morphological properties of ESO 598-G009, NGC 1515 and NGC 7456, using the isophotal maps which are made from density maps on SAOimage which allows easy identification of detailed features. In all the isophotal maps, the interval of contours is 0.5 mag arcsec^{-2} and top is to the north and left is to the east.

We have used the ellipse fitting method in SPIRAL to determine the luminosity profiles along the major axis together with the ellipticity and position angle of each isophote. In the ellipse fitting method, the observed isophotes are fitted to sets of concentric ellipses. Position angle of each isophote is defined as the angle measured counter-clockwise from the north to the direction of the isophote's major axis and its ellipticity is 1 - b/a where a and b are the semi-major and semi-minor axes.

Generally the luminosity of a galaxy is composed of the luminosities from bulge and disk components. It is commonly known that the luminosity profile of bulge follows de Vaucouleurs' law and that of disk follows exponential law (Freeman 1970). We can decompose observed luminosity into bulge and disk components using the iterative decomposition method, which was described in Choi et al. (1993).

III. PHOTOMETRIC RESULTS

(a) ESO 598-G009

The B-band image of ESO 598-G009 given in Figure 1(a) shows a bright bulge and ring shape, but does not show clear spiral structure. Although this galaxy is classified as Sb(pec), we can also find the existence of low-surface-brightness arcs or plume which is face-on or near face-on sheets at north (Schombert et al. 1990).

The structure is illustrated by the isophotal map in Figure 2. Each tick in ordinate and abscissa represents 12.44″. The innermost contour levels are 21.0, 20.0, 19.5 and 18.5 mag arcsec^{-2} respectively for B-, V-, R- and I-bands. In all bands an intermediate region between bulge and disk including a ring shape is clearly shown. The isophotal maps in B-, V- and R-bands show that the southern region of disk is larger than the northern region, while the isophotal map in I-band shows the opposite.

We can see the clockwise isophotal twist which may be due to the spiral structure, which is supported by the decreasing position angle profiles (Fig. 3) up to 40″

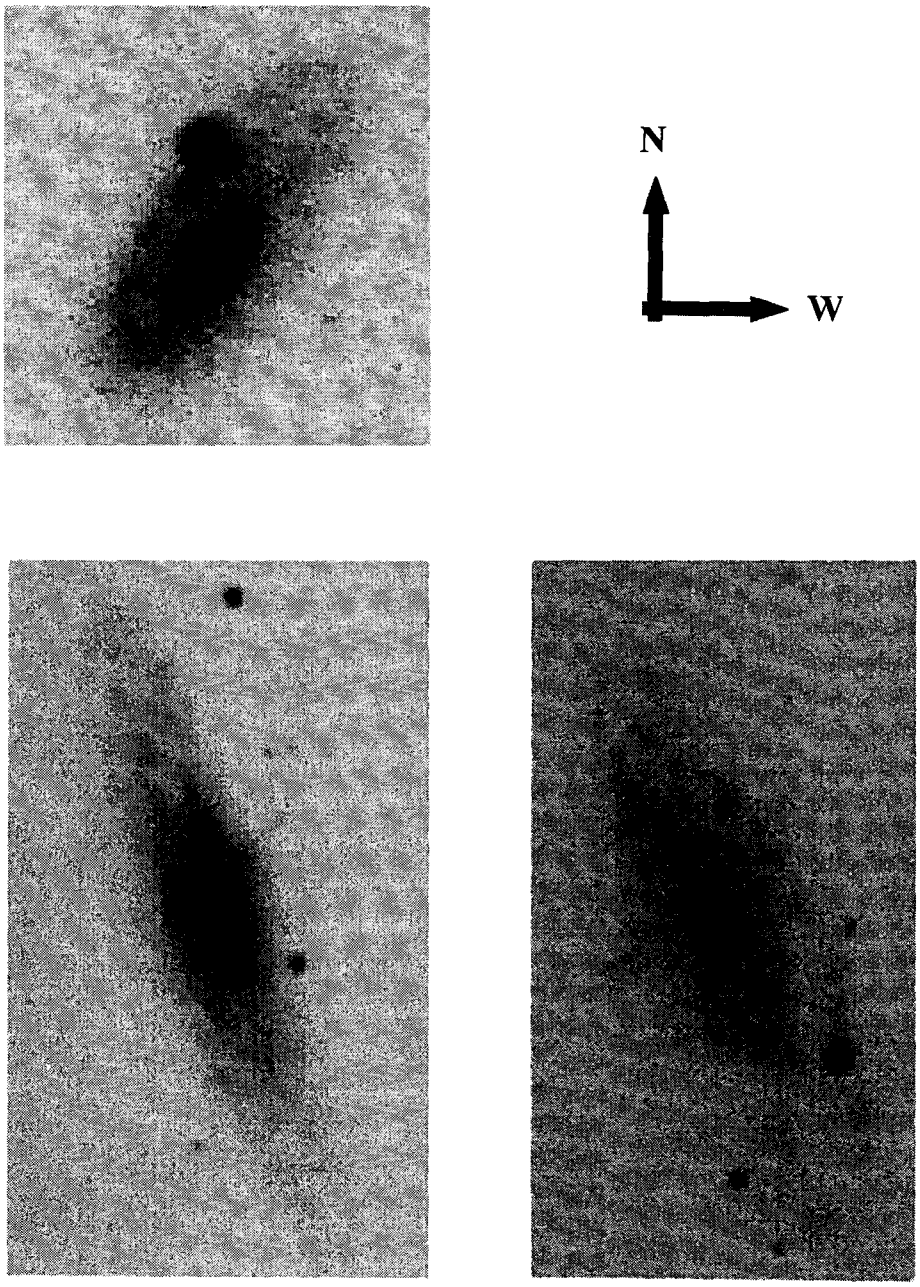

Fig. 1.— The B-band images of (a)ESO 598-G009, (b)NGC 1515 and (c)NGC 7456.

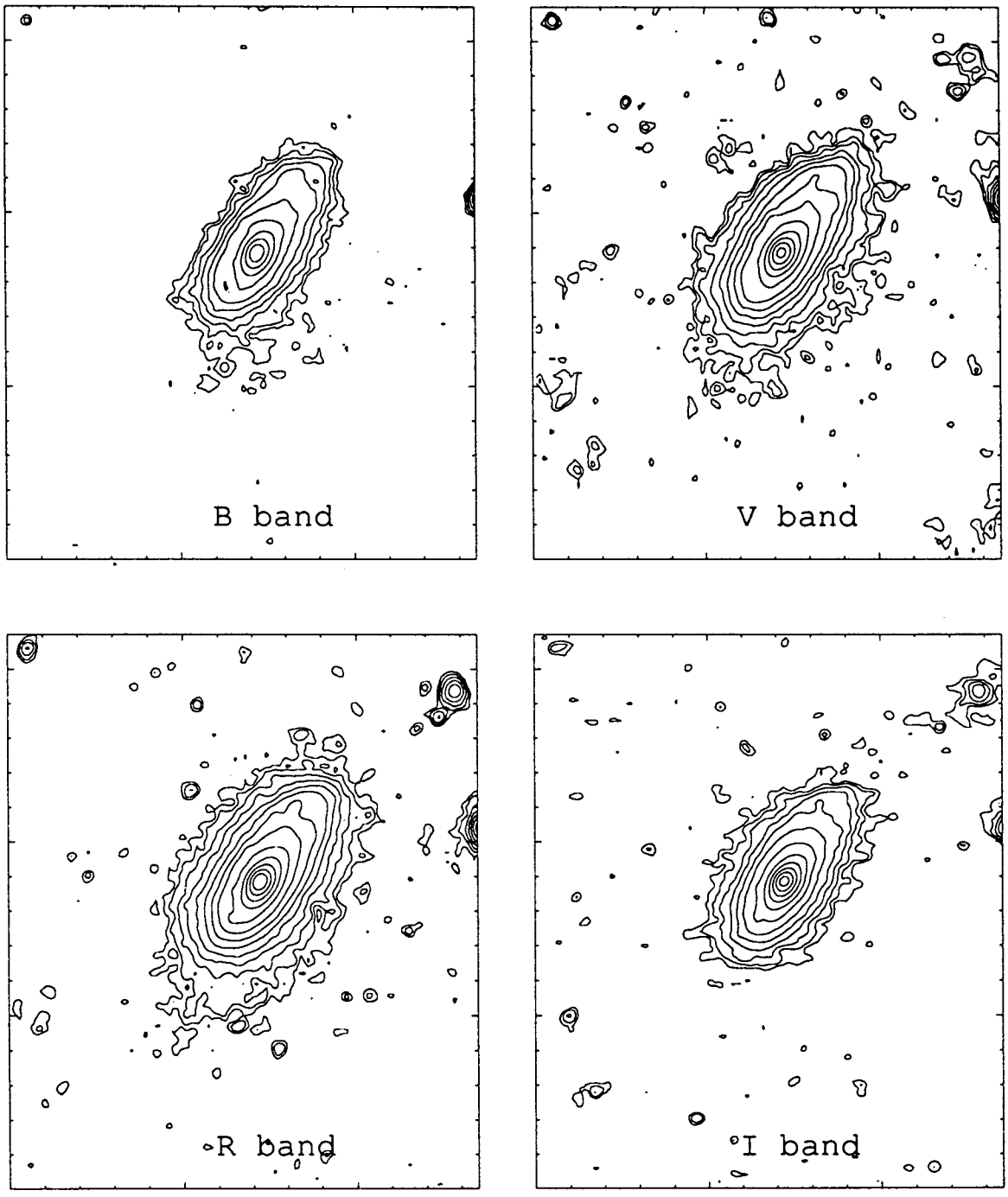

Fig. 2.— Isophotal maps of ESO 598-G009 in B-, V-, R- and I-bands. One tick indicates 12.44″ (*The top is north and the left is east*). The step of the isophotes is 0.5 mag arcsec^{-2} ; the outmost isophotes are 26.0 mag arcsec^{-2} in B- and V-bands, 25.5 mag arcsec^{-2} in R-band and 19.5 mag arcsec^{-2} in I-band.

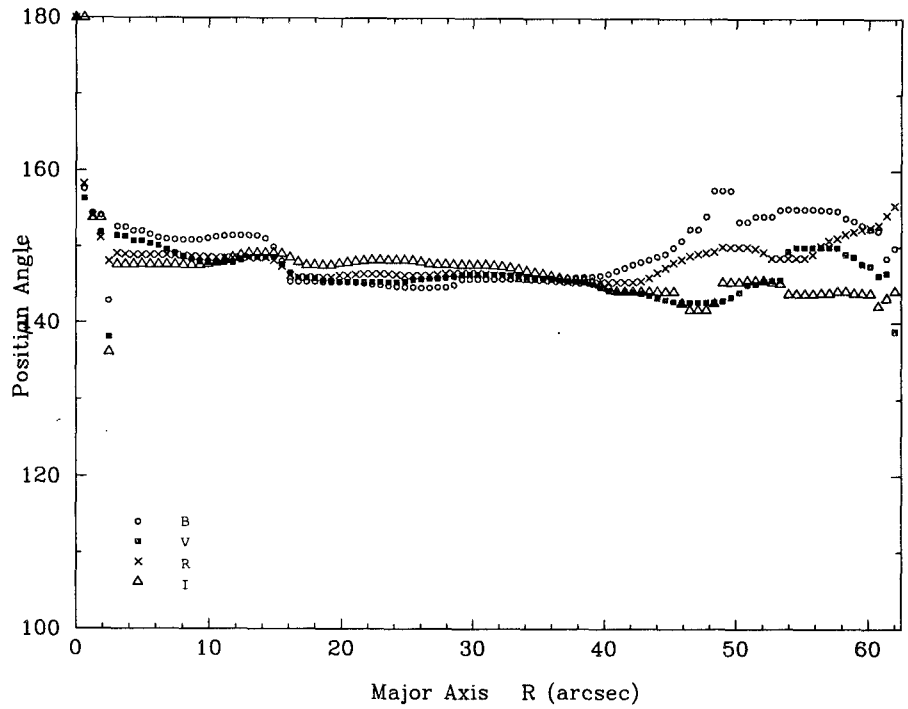

Fig. 3.— Position angle profiles of ESO 598-G009 along the major axis in B-, V-, R- and I-bands.

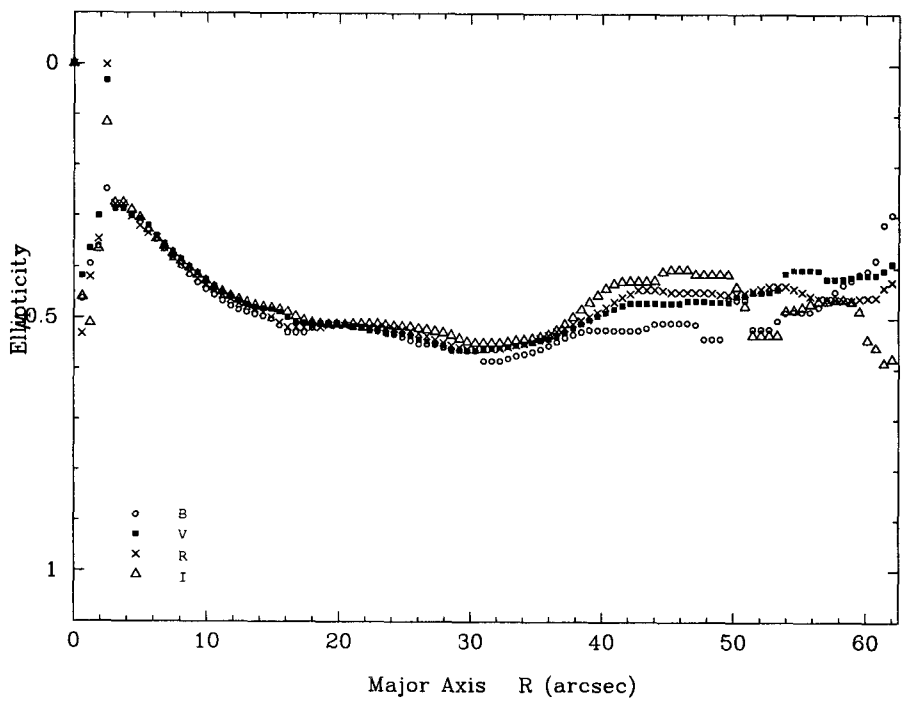

Fig. 4.— Ellipticity profiles of ESO 598-G009 along the major axis in B-, V-, R- and I-bands.

from the galactic center. In the same region, however, the position angles have a little different values in each band, while the ellipticity profiles (Fig. 4) have the same features in all bands. Especially, the change of the profiles is conspicuous at the intermediate region (R $\sim$ 15″).

The position angle and ellipticity have the same value in all bands at R $\sim$ 35″. This may be another evidence of the existence of a ring in this galaxy. At R > 40″, the position angle profiles definitely increase in B- and R-band and the ellipticity profiles have the lower values at bluer bands. These might be related to the plume or arc shape.

The luminosity profiles along the major axis are given in Figure 5. In all bands, the rising of luminosity at ring-like region (R $\sim$ 35″) is seen. At R > 40″, however, another rising of luminosity at R > 45″ is shown in all bands except for I-band which is very noisy.

$B - V$ and $V - I$ color profiles and color contour maps whose ticksize is the same as that in the isophotal maps are given in Figures 6 and 7. $B - V$ and $V - I$ color profiles become gradually getting bluer from center to outer region and become more rapidly bluer at R > 40″, while the outermost redder region and red dip in $V - I$ color are due to photometric error such as the estimation error of disk boundary and the noise of luminosity in I-band. In general, this getting bluer pattern in the outer part of spiral galaxy has been thought to be mainly due to young stellar populations (Tinsley and Larson 1978). By Reduzzi and Rampazzo (1996), rings tend to be bluer than the nearby parts of the galaxy. However the ring region (R $\sim$ 35″) shows the redder color in Figure 6, which may be due to the dust. The outskirt except western regions shows bluer color in $B - V$ contour image and the western and northeastern regions shows bluer color in $V - I$. The plume region, at R $\sim$ 40″, has $B - V$ color of 0.7, which is consistent with Schombert et al. (1990).

Figure 8 shows the result of the profile decomposition. The dot-dashed line indicates the luminosity of bulge, the dashed line presents the luminosity of disk and the solid line indicates the combined luminosity of the two components. It is difficult to decompose the luminosity profile in I-band because of the low signal-to-noise ratio of disk.

The decomposition profiles show a depression between R $\sim$ 7″ and R $\sim$ 16″, which is accentuated by comparison with the following hump between R $\sim$ 25″ and R $\sim$ 35″ caused by the spiral arms. These features give an appearance of the type II disk of Freeman (1970), which have been explained by the presence of a lens (Freeman 1977), or by an inner cutoff in the disk (Kormendy 1977a), or by a bulge that does not follow the de Vaucouleurs law in all its extension (Boroson 1981), or by the combined effect of enhanced young stellar population and its associated dust (Prieto et al. 1992). However, Marquez and Moles (1996) pointed out that the type II profiles can be shown in the interacting galaxies.

The total integrated magnitudes are 12.30, 10.73, 10.45 and 10.53 for B-, V-, R-, and I-band, respectively.

(b) NGC 1515

NGC 1515 is a highly inclined intermediate type barred spiral galaxy as shown in Figure 1(b). It has a peanut or box shape bulge (Combes et al. 1990) and two spiral arms. Isophotal maps of the NGC 1515 are presented in Figure 9. The ticksize is 18.72″ along the vertical and 18.25″ along the horizontal axis. The innermost contour levels are 21.0, 20.0, 19.0 and 18.5 mag arcsec^{-2} for B-, V-, R-, and I-band respectively.

The bulge shows an asymmetric shape and the outer contours of the bulge are more rectangular than ellipse. There are isophotal twists in the isophotes of the bulge. There seems to be a bar component whose major axis is not aligned to the disk major axis.

Position angle profile (Fig.10) shows the similar pattern in all bands, which has an ascent and descent from the center to R $\sim$ 30″. In this region, however, the maximum change of position angle occurs in I-band while the minimum occurs in B-band. The increase of position angle due to the spiral structure is shown at R $\gtrsim$ 40″ in all bands. In all bands, the flat region (20″ < R < 30″) is the evidence of bar. It is shown in Figure 11 that the contours are gradually flattened except for the central region which is mentioned in the position angle profile.

In I-band, when the ellipticity has the maximum value at R $\sim$ 11″, the position angle has 21° which is maximum difference with respect to that of bar. Isophotal twist in the central region can be explained by three different mechanisms. Shaw et al. (1993) suggested that leading gas shocks inside the inner Lindblad resonance (ILR) distort the stellar orbits and cause an inner twisted region at some fixed orientation relative to the bar. Friedli & Martinet (1993) and Wozniak et al. (1995) suggested that the inner twisted region is a second, independently moving bar. Twists might also be the result of triaxial bulges (Kormendy 1979).

The luminosity profiles (Fig. 12) show two dips of luminosities, which are the region around R $\sim$ 60″ and R $\sim$ 120″ and prominent in B-band. The rising of the luminosity which may be due to spiral structure is seen at R > 110″ in all bands.

$B - V$ and $V - I$ color profiles along the major axis (Fig. 13) show a small gradient from galactic center to disk. However, the red color is seen in central and outermost regions and the blue bumps are seen in the same region that the luminosity dips are seen. $B - V$ and $V - I$ color maps show the asymmetric color pattern and blue color near spiral arms (Fig.14).

In order to understand the reason for the dips in Figure 12, we plotted the luminosity distribution along

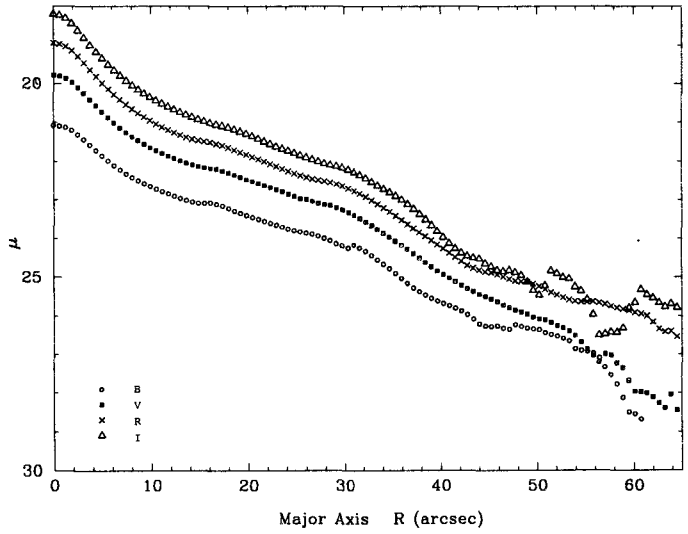

Fig. 5.— Luminosity profiles of ESO 598-G009 along the major axis in B-, V-, R- and I-bands.

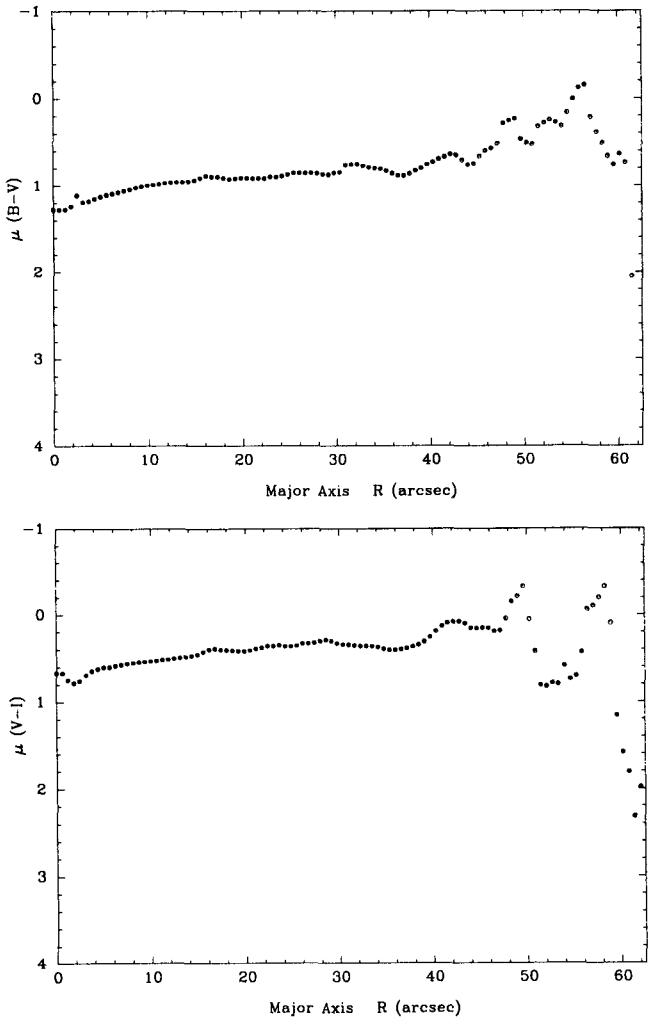

Fig. 6.— $(B - V)$ and $(V - I)$ color profiles of ESO 598-G009.

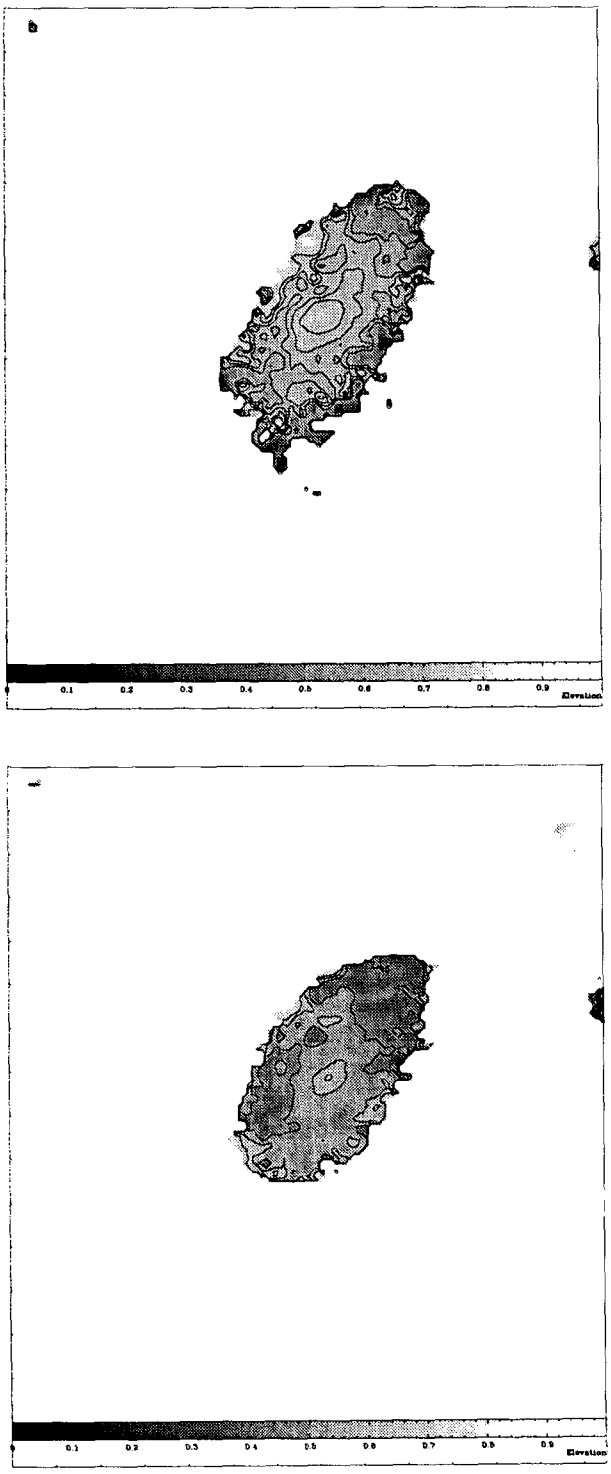

Fig. 7.— $(B-V)$ and $(V-I)$ color contour maps of ESO 598-G009 (*The top is north and the left is east*). The contour level is 0.8, 0.9, 1.0 and 1.1 in $(B-V)$ color and 0.4, 0.6 and 0.8 in $(V-I)$ color.

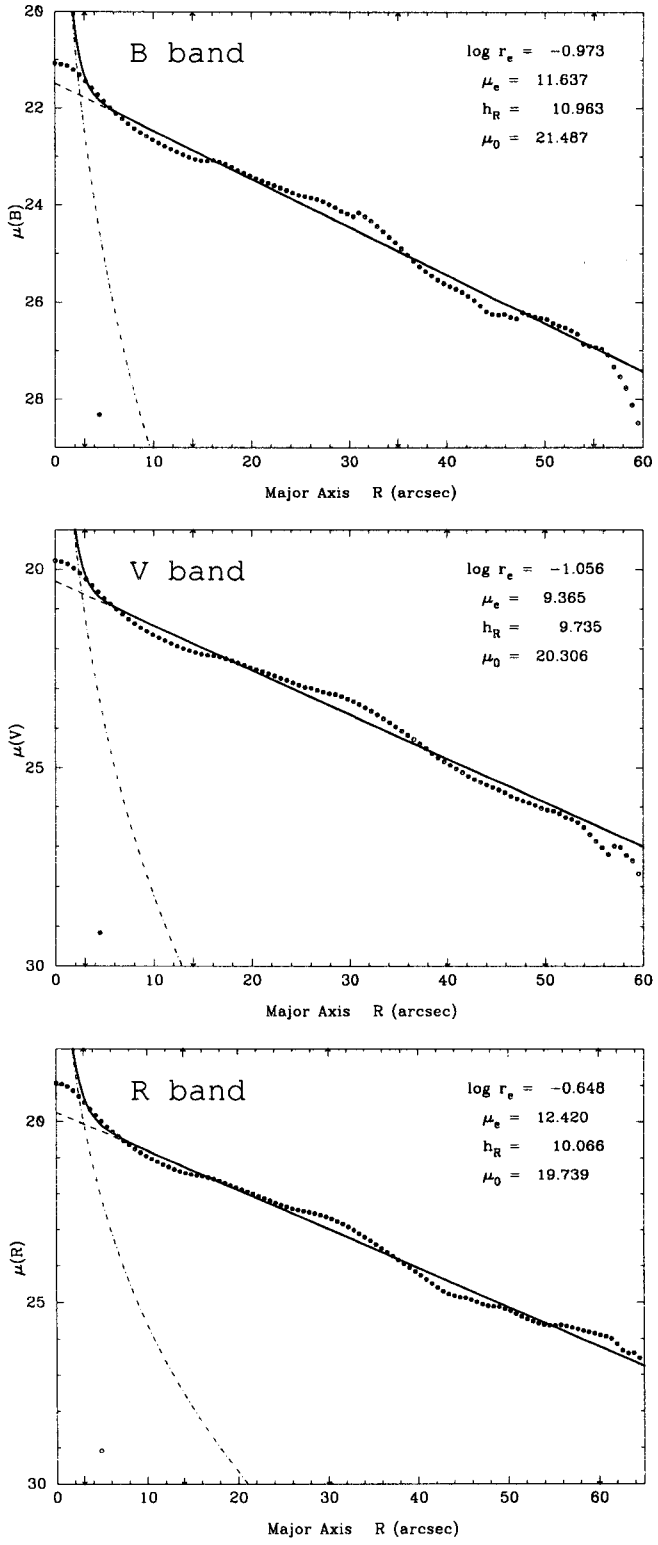

Fig. 8.— Luminosity profile decompositions of ESO 598-G009 in B-, V- and R-bands.

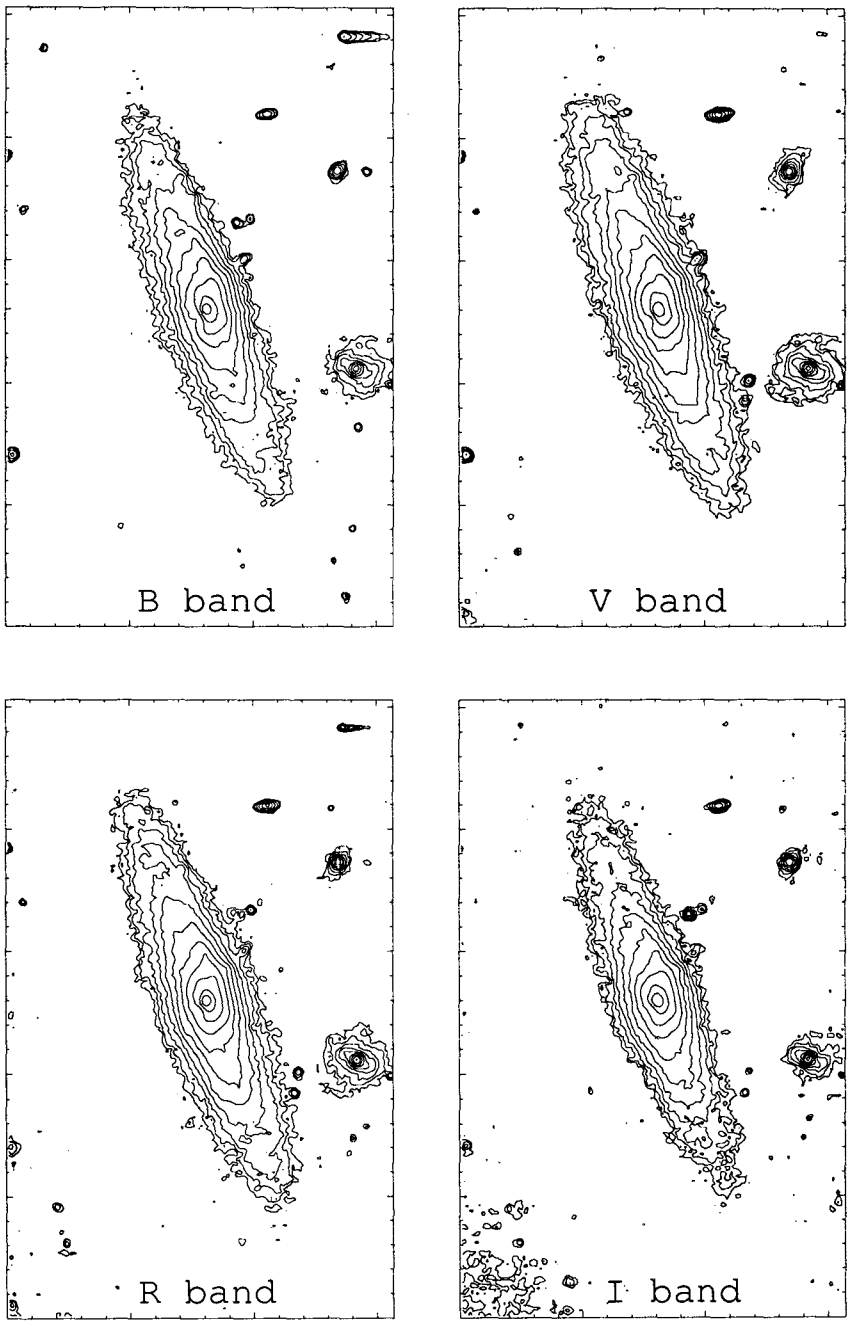

Fig. 9.— Isophotal maps of NGC 1515 in B-, V-, R- and I-bands. Vertical tick indicates 18.72″ and horizontal tick 18.25″. The step of the isophotes is 0.5 mag arcsec^{-2}; the outmost isophotes are 25.5, 25.0, 24.0 and 23.0 mag arcsec^{-2} respectively for B-, V-, R-, and I-bands.

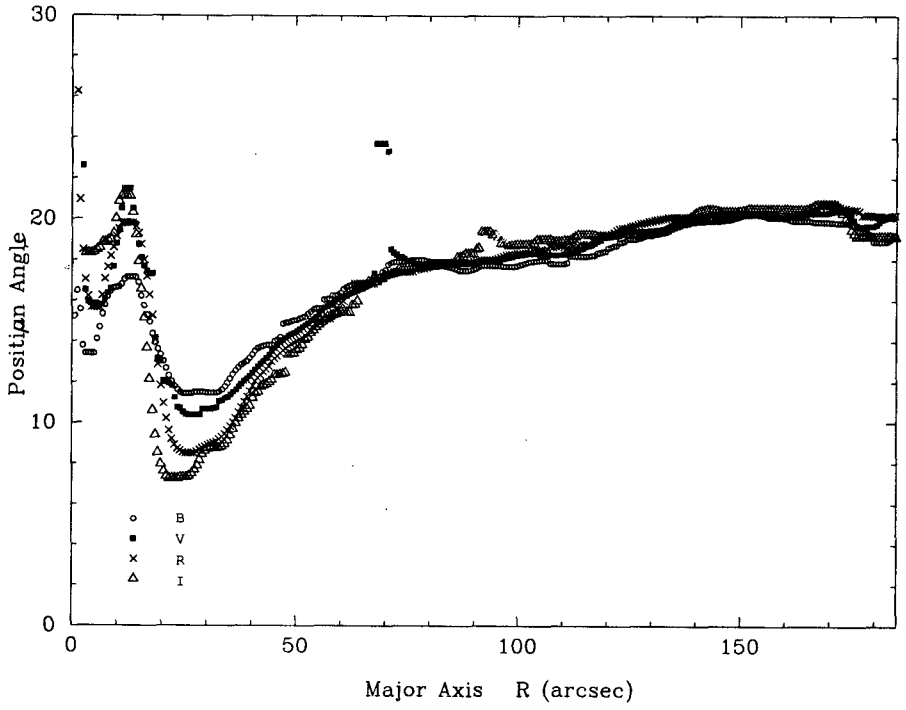

Fig. 10.— Position angle profiles of NGC 1515 along the major axis in B-, V-, R- and I-bands.

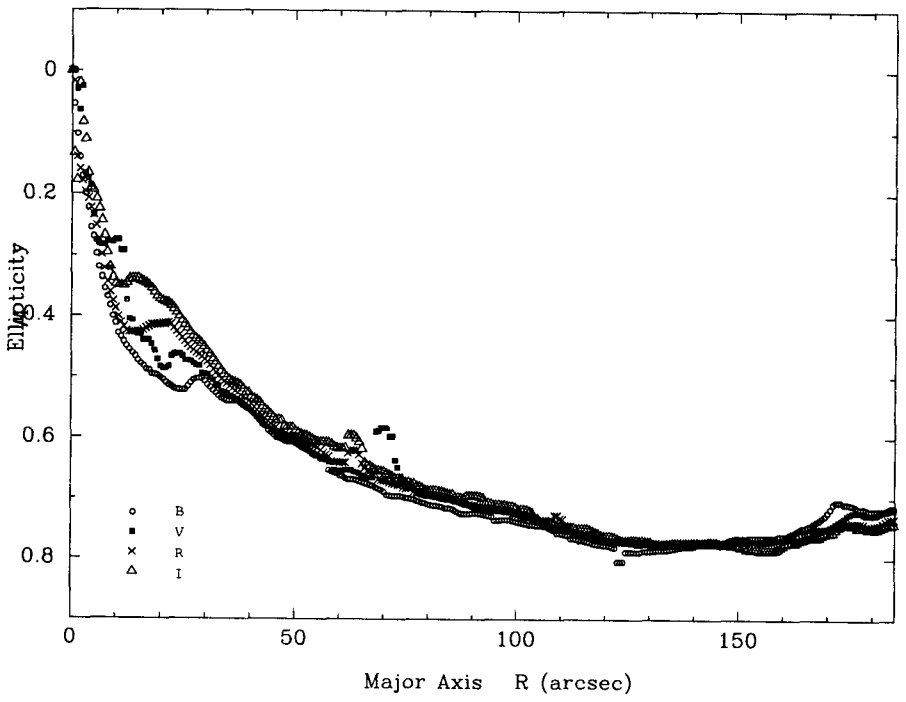

Fig. 11.— Ellipticity profiles of NGC 1515 along the major axis in B-, V-, R- and I-bands.

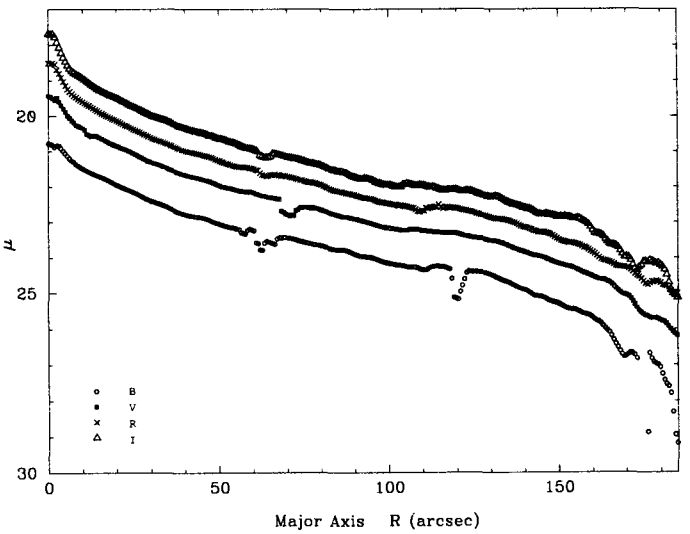

Fig. 12.— Luminosity profiles of NGC 1515 along the major axis in B-, V-, R- and I-bands.

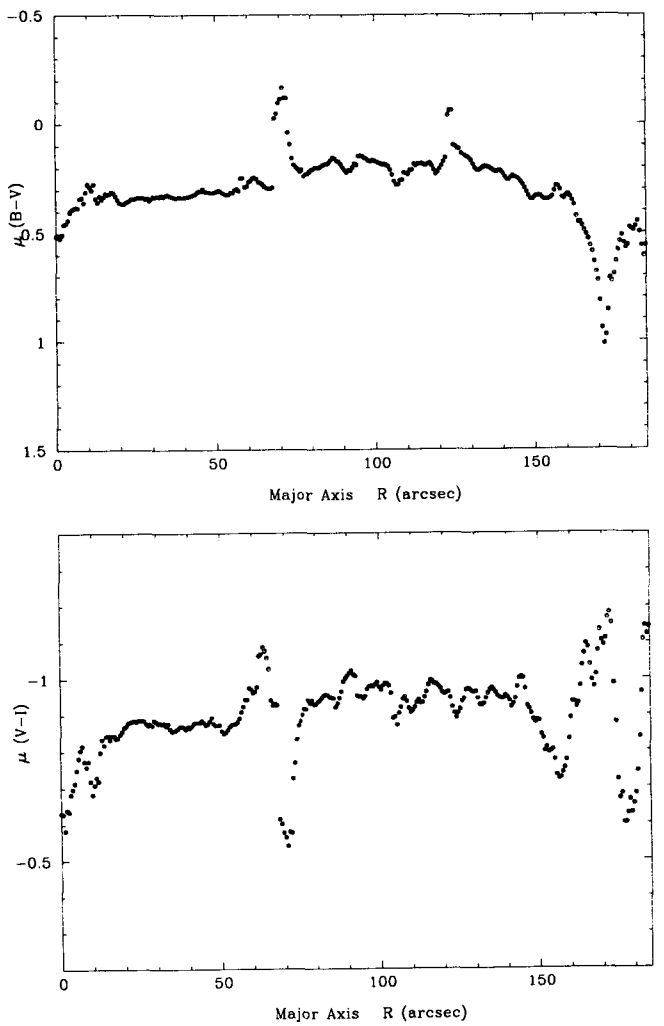

Fig. 13.— $(B - V)$ and $(V - I)$ color profiles of NGC 1515.

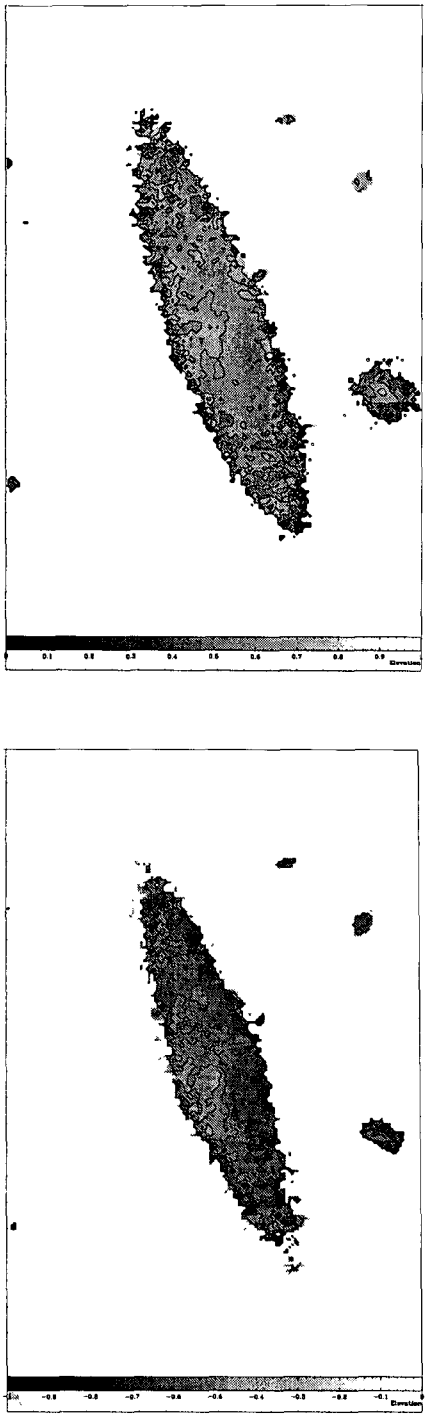

Fig. 14.— $(B-V)$ and $(V-I)$ color contour maps of NGC 1515. The contour level is 0.0, 0.2, 0.4 and 0.6 in $(B-V)$ color and -1.0, -0.8, -0.6 and -0.4 in $(V-I)$ color.

the major and minor axes. At R $\sim$ 60″ and 120″ , the luminosity profile along northeast major axis has the prominent dip in B-band. The bumps and dip in $B-V$ and $V-I$ color profiles could be explained by dust lane. We can see that the luminosity at northwest minor axis is higher than at southeast minor axis, which means highly inclinated large bulge.

The decomposed profile (Fig.16) shows the type I profile of Freeman (1970) and the luminosity bump at 100″ $\lesssim$ R $\lesssim$ 160″ due to the luminosity of the well-developed spiral arm. Because of the heavy contamination by the luminosity of spiral arms, the luminosity bumps are shown in all bands. Using these photometric parameters, we could derive the bulge-to-disk luminosity ratio in magnitude as 2.36 in B-band. This value corresponds to the morphological type between T=4 and T=5 according to Simien & de Vaucouleurs (1986). The integrated magnitudes are 10.45, 9.51, 11.08 and 10.67 for B-, V-, R-, and I-band, respectively.

(c) NGC 7456

NGC 7456, shown in Figure 1(c), has a very small nucleus and no central bulge as in other Sc galaxies with low central surface brightness of disk. The spiral arms are multiple and fragmentary, which is known as flocculent spiral structure by Elmegreen and Elmegreen (1982).

Isophotal maps of the NGC 7456 are presented in Figure 17. The ticksize is 18.6″, and the innermost contour levels are 22.5, 21.5, 21.0 and 20.0 mag arcsec^{-2} respectively for B-, V-, R- and I-bands. We can see a small nucleus and spiral structures. In B-band disk, the blue spots which are suspected to be HII regions are shown.

Position angle profiles (Fig.18) show slight decrease pattern with a rapid increase in the central region (R < 15″). Stark (1977) showed that the position angle along radius is changed in triaxial bulge. At R < 15″, the change of the position angle seems to reflect the triaxiality of the nuclear component. Ellipticity of the nucleus is 0.3, as shown in Figure 19, while that of the disk region is nearly constant.

We can see the luminosity profile (Fig. 20) which shows very small bulge component and that most of the galaxy luminosity comes from the disk luminosity. There are strong signs for spiral arm components which are looked like a saw teeth, especially in B-band.

$B-V$ color profile along the major axis (Fig.21) shows nearly constant colors in R < 20″ and becomes bluer slightly with increasing radius up to R $\sim$ 50″. $V-I$ color profile shows generally the same trend with $B-V$ color except in the outer region. The opposite pattern in outer region is due to the low signal-to-noise ratio in redder bands. The color maps in Figure 22 shows the same trend as in Figure 21. We could not find any evidence of HII region (Sandage & Brucato 1979) which might be confirmed from the observations in Hα band.

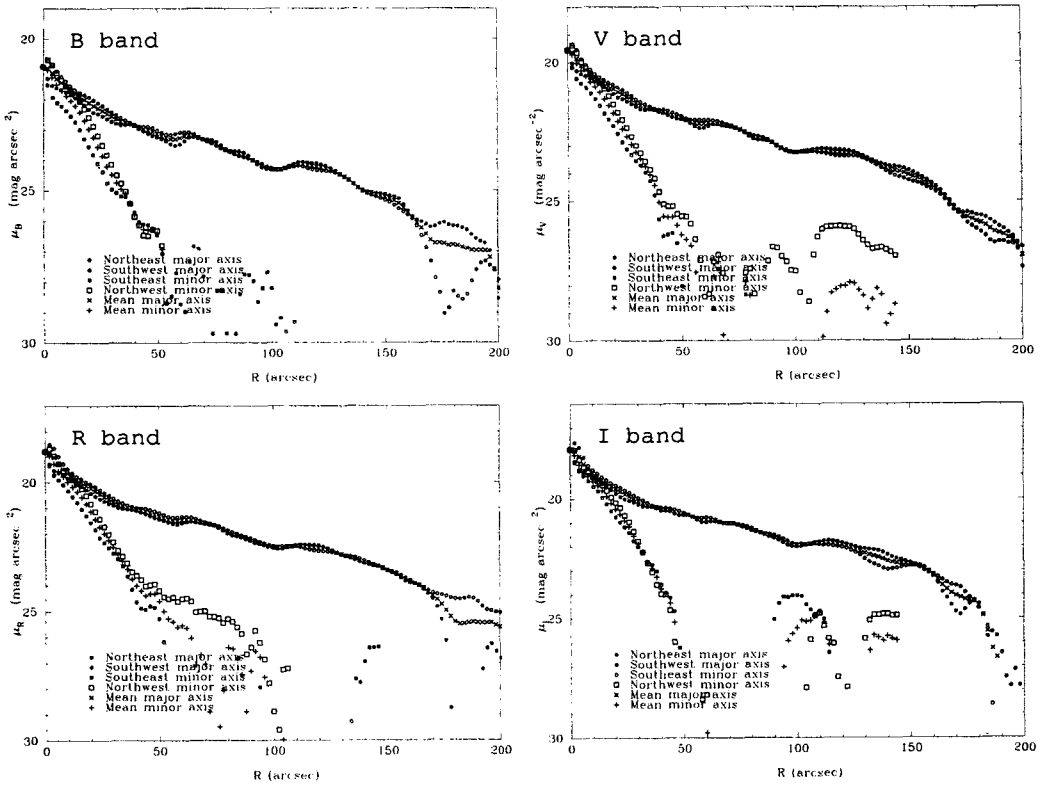

Fig. 15.— The luminosity profile of NGC 1515 along the major and minor axes in B-, V-, R- and I-bands.

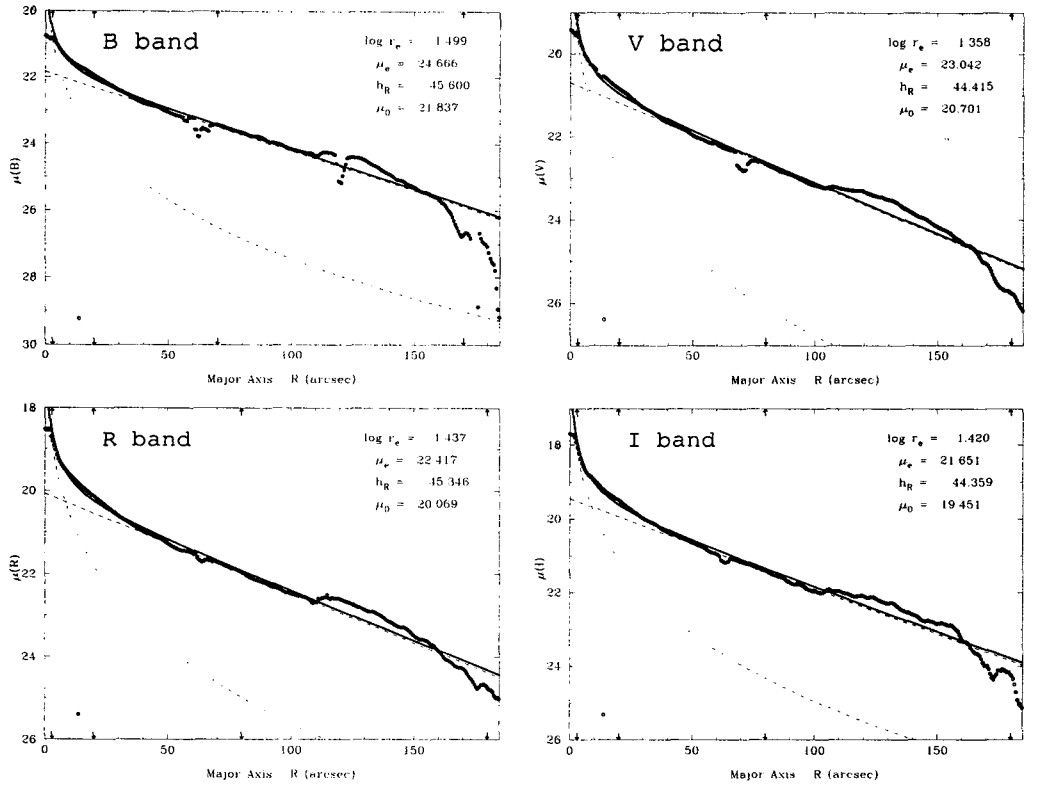

Fig. 16.— Luminosity profile decompositions of NGC 1515 in B-, V-, R- and I-bands.

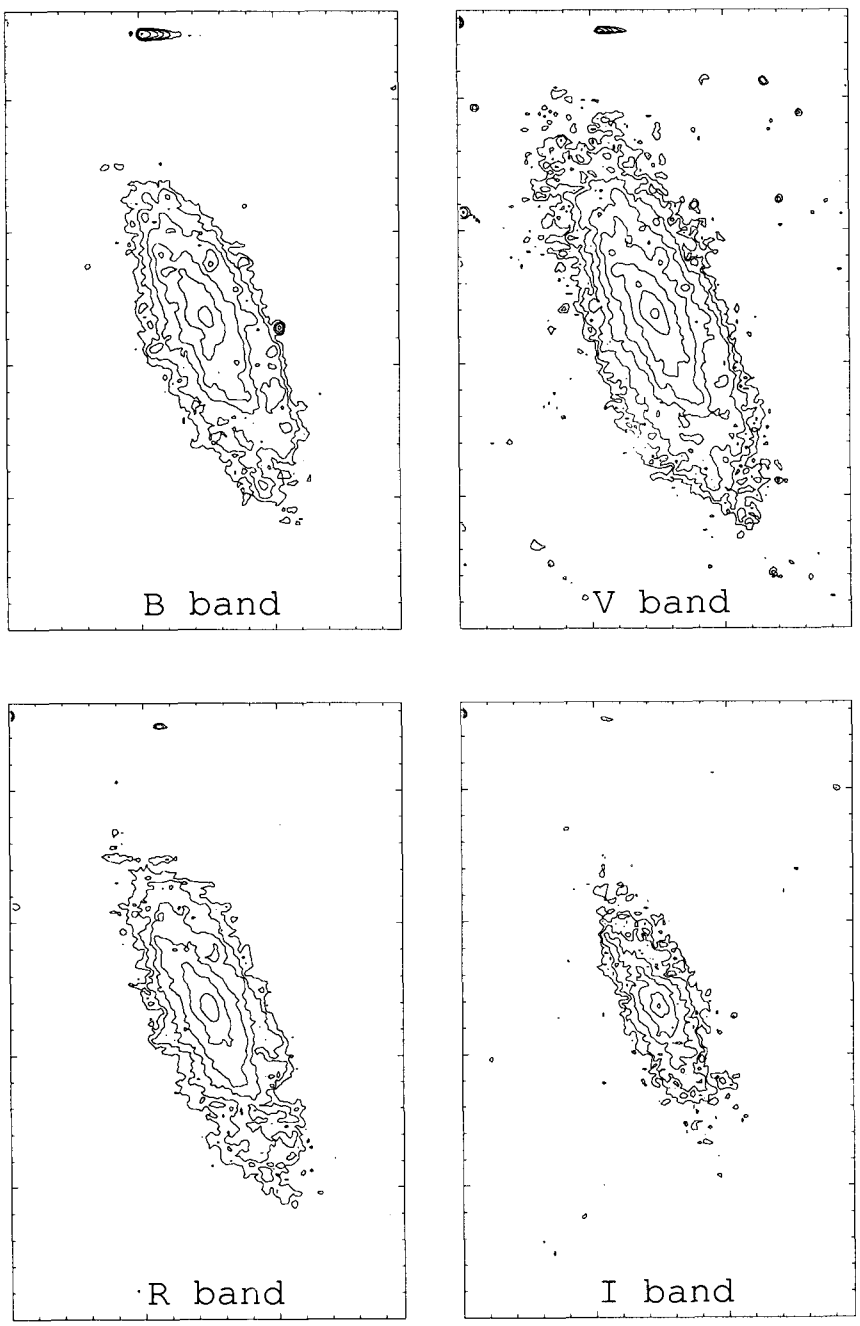

Fig. 17.— Isophotal maps of NGC 7456 in B-, V-, R- and I-bands. One tick indicates 18.6″. The step of the isophotes is 0.5 mag arcsec^{-2} ; the outmost isophotes are 25.0 mag arcsec^{-2} in B- and V-band, 23.5 in R-band and 22.5 in I-band.

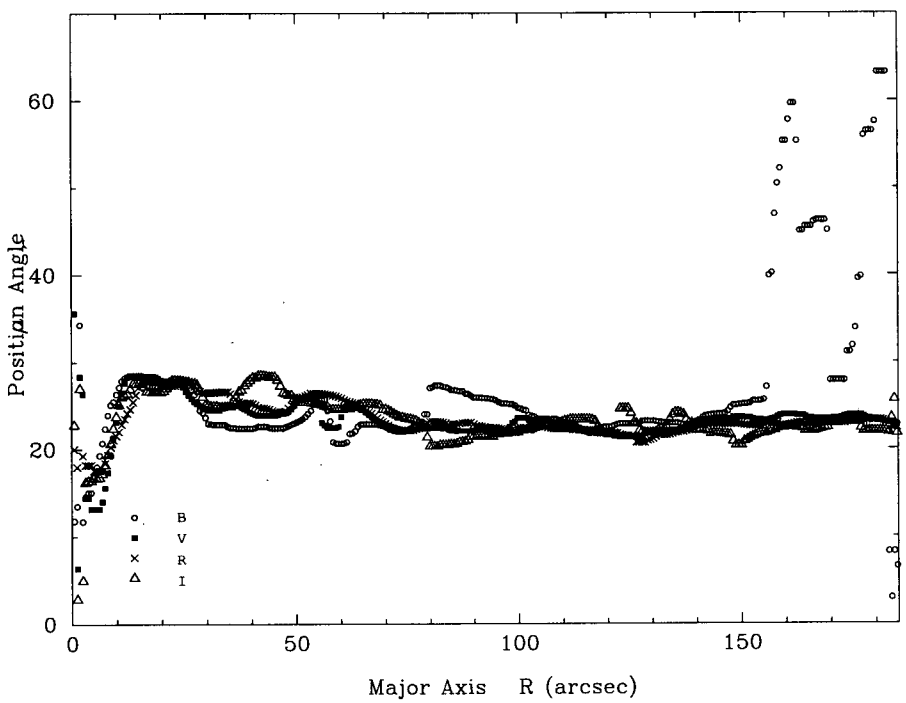

Fig. 18.— Position angle profiles of NGC 7456 along the major axis in B-, V-, R- and I-bands.

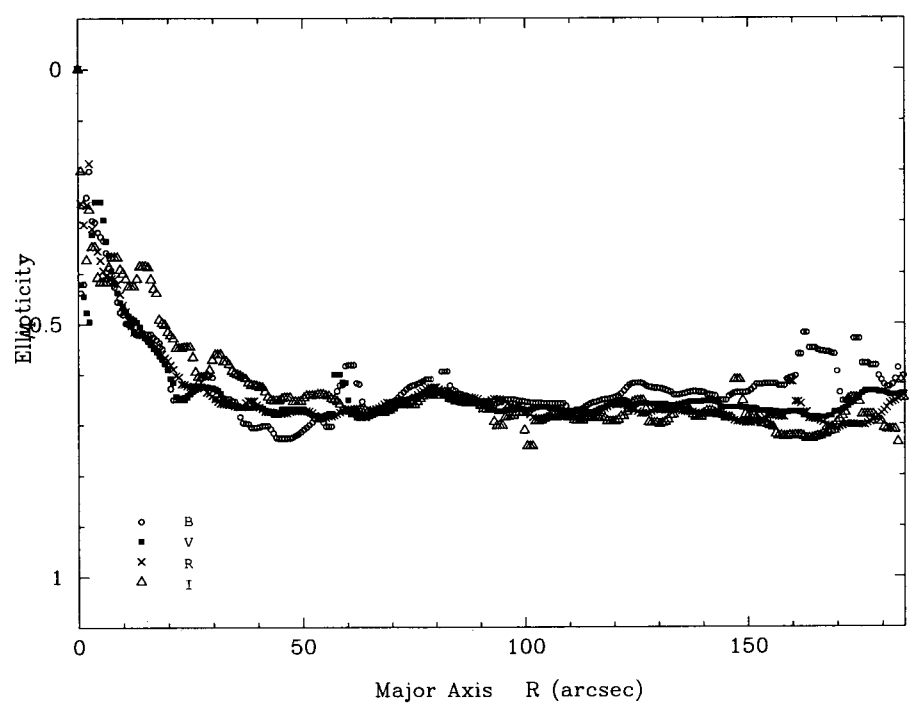

Fig. 19.— Ellipticity profiles of NGC 7456 along the major axis in B-, V-, R- and I-bands.

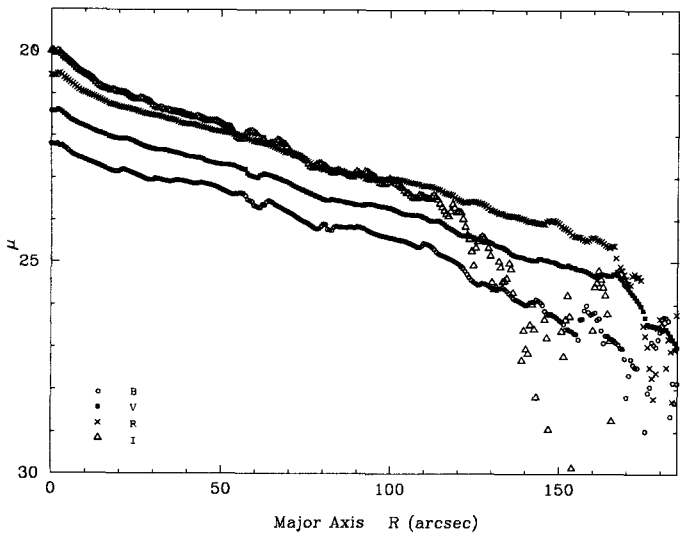

Fig. 20.— Luminosity profiles of NGC 7456 along the major axis in B-, V-, R- and I-bands.

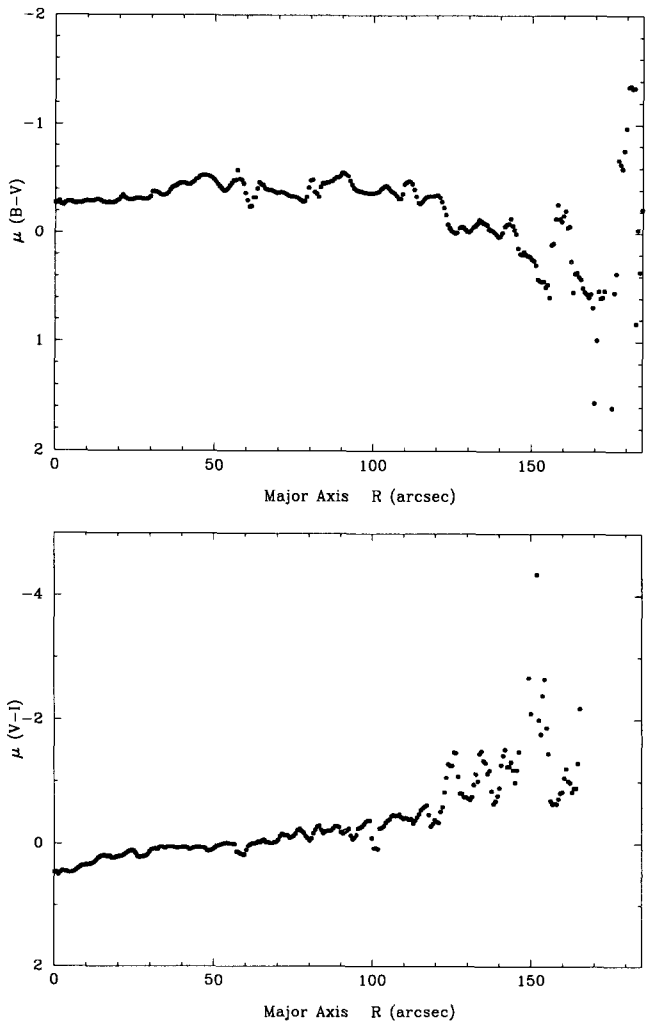

Fig. 21.— $(B - V)$ and $(V - I)$ color profiles of NGC 7456.

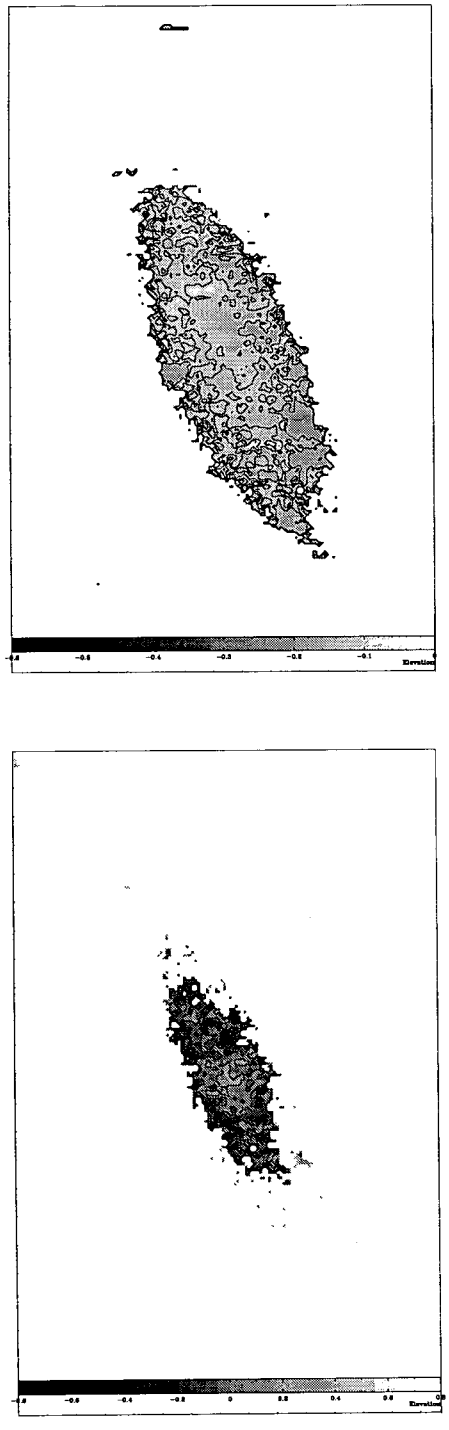

Fig. 22.— $(B-V)$ and $(V-I)$ color contour maps of NGC 7456. The contour level is -0.6, -0.4, -0.2 and 0 in $(B-V)$ color and -0.2, 0, 0.2 and 0.4 in $(V-I)$ color.

The result of the luminosity decomposition (Fig. 23) shows a very small nucleus and exponential disk which is affected by multiple spiral arms. The bulge-to-disk ratio is 4.19 in B-band which corresponds to the morphological type T=6 (Simien & de Vaucouleurs 1986). The integrated magnitudes are 10.96, 10.76, 11.10 and 12.78 for B-, V-, R-,and I-band, respectively.

IV. DISCUSSION

The depression between R $\sim$ 7″ and R $\sim$ 16″, seen in the luminosity profile of ESO598-G009 (Fig. 8) suggests the type II disk of Freeman (1970) for the disk of ESO598-G009, which is thought to be caused by the secular evolution driven by bar (Ann 1997) or by the interaction with companion galaxies (Marquez and Moles 1996). Using statistical analysis, Soares et al. (1995) suggested that ESO 598-G009 is a binary system with the companion ESO 598-G011, which is an Sc type galaxy located at the southeast with respect to ESO 598-G009. Because the redshift information of ESO 598-G011 is not known, it is not possible to figure out whether or not ESO 598-G011 is a gravitational companion of ESO 598-G009.

The dips in the luminosity profiles of NGC 1515 (Fig. 12) are thought to be caused by dust lanes which is also apparent in the $B-V$ and $V-I$ color profiles. The isophotal twists observed in the isophotal maps of NGC 1515 (Fig. 9) indicate that the bulge of NGC 1515 is triaxial. The origin of the triaxial bulge is not clearly understood but the presence of the inner Lindblad resonance (ILR) is a crucial to derive secular evolution which leads to triaxial bulge (Shaw et al. 1993; Wozniak et al. 1995).

V. SUMMARY

Through this study we have investigated various properties for the galaxies of ESO 598-G009, NGC 1515 and NGC 7456. The main properties are summarized as follows.

ESO 598-G009, classified as Sb(pec), shows a bright bulge and a ring. There seems to be a trace of the gravitational interaction, such as a plume in the surface brightness.

NGC 1515 is a spiral galaxy with a bar which is apparent in the isophotal maps and in the position angle profile. Its bulge-to-disk ratio, $\Delta\mu$, is 2.36 which is a typical value for the galaxies with morphological type Sbc or SBbc (Simien & de Vaucouleurs 1986). There is a dust lane in northeast part of the galaxy.

NGC 7456 is a late type spiral galaxy with very small bulge-to-disk ratio, $\Delta\mu = 4.19$ which corresponds to the morphological type T=6 or late. Although NGC 7456 has very blue color, there is no clear evidence of HII regions.

ACKNOWLEDGEMENTS

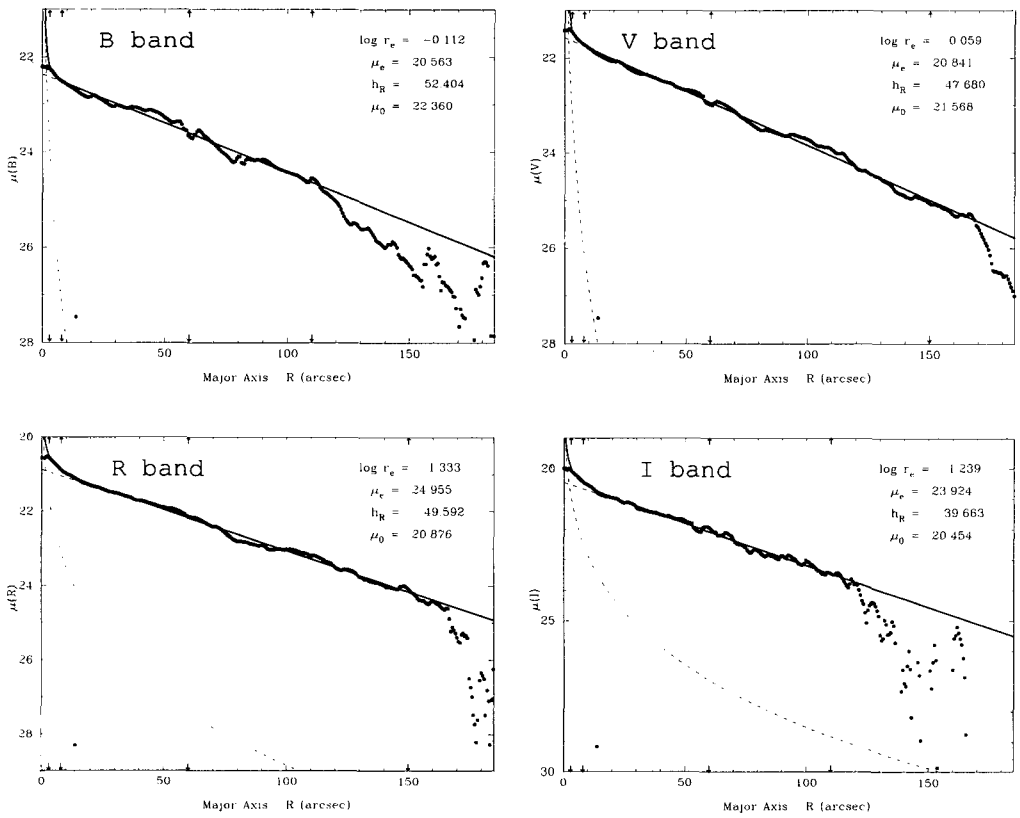

Fig. 23.— Luminosity profile decompositions of NGC 7456 in B-, V-, R- and I-bands.

B. G. Park thanks the staff of MSSSO for their kind support during the observation period in September 1993. This wrok was supported in part by the Basic Science Research Program, BSRI-97-5411.

REFERENCES

Ann, H. B., 1997, JKAS, 30, 165

Ann, H. B., & Lee, S. W., 1987, JKAS, 20, 49

Boroson, T., 1981, ApJS, 46, 177

Burstein, D., 1979, ApJS, 41, 435

Choi, J. T., Ann, H. B., & Lee, H. M., 1993, JKAS, 26, 33

Combes, F., Debbasch, F., Friedli, & Pfenniger, D., 1990, A&A, 233, 82

Elmegreen, D. M. & Elmegreen, B. G., 1982, MNRAS, 201, 1021

Freeman, K. C., 1970, ApJ, 160, 811

Freeman, K. C., 1977, IAU Symposium 77, Structure and Properties of Nearby Galaxies, eds. E.M. Berkhuijsen, R. Wielebinski (Reidel, Dordrecht) 3

Friedli, D., & Marinet, L., 1993, A&A, 277,27

Ichikawa, S., Okamura, S., Watanabe, M., Hamabe, M., Aoki, T. & Kodaira, K. 1987, Annals Tokyo Astr. Obs., 21, 285

Kent, S. M., 1985, ApJS, 59, 115

Kormendy, J., 1977a, ApJ, 217, 406

Kormendy, J., 1977b, ApJ, 241, 359

Kormendy, J., 1979, ApJ, 227, 714

Lauberts, A., 1982, *The ESO/Uppsala Survey of the ESO(B) Atlas* (ESO)

Marquez, I., & Moles, M., 1996, A&AS, 120, 1

Mathewson, D. S., Ford, V. L., & Buchhron, M., 1992, ApJS, 81, 413

Mathewson, D. S., & Ford, V. L., 1996, ApJS, 107, 97

Park, B.-G., 1993, *A CCD Surface Photometric Study of Extra-galaxies*, Minitry of Science and Technology

Reduzzi, L., & Rampazzo, R., 1996, A&AS, 116, 515

Prieto, M., Beckmann, J. E., Cepa, J. & Varela, A. M., 1992, A&A, 257, 85

Sandage, A., & Brucato, R., 1979, AJ, 84, 472

Sandage, A., & Tammann, G. A., 1981 *Carnegie Institution of Washington Publication*, 635 (RSA)

Shaw, M. A., Combes, F., Axon, D. J., & Wright, G. S., 1993, A&A, 273, 31

Schombert, J., Wallin J. F., & Struck-Marcell, C., 1990, AJ, 99, 497

Simien, F., & de Vaucouleurs, G, 1986, ApJ, 302, 564

Soares, D. S. L., de Souza, R. E. de Carvalho, R. R., & Couto da Siva, T. C., 1995, A&AS, 110, 371

Stark, A. A., 1977, ApJ, 213, 273

Tinsley, B. M. & Larson, R. B., 1978, ApJ, 221, 554

de Vaucouleurs, G., de Vaucouleurs, A., Corwin Jr., H. G., Buta, R. J., Paturel, G., & Fouque, P., 1991, *Third Reference Catalogue of Bright Galaxies* (RC3)

Vorontsov-Vel'yaminov, B., 1977, ApJS, 28, 1 (MCG)

Wozniak, H., Friedli, D., Martinet, L., Martin, P., & Bratschi, P., 1995, A&AS, 111, 115